

Automatic Recognition of Boredom in Video Games Using Novel Biosignal Moment-Based Features

Dimitris Giakoumis, Dimitrios Tzovaras, *Member, IEEE*,
Konstantinos Moustakas, *Member, IEEE*, and George Hassapis, *Senior Member, IEEE*

Abstract—This paper presents work conducted toward the biosignals-based automatic recognition of boredom, induced during video-game playing. For this purpose, common biosignal feature extraction methods were exploited and their capability to identify boredom was assessed. Moreover, for the first time, Legendre and Krawtchouk moments, as well as novel moment variations, were extracted as biosignal features and their potential toward automatic affect recognition was examined using the specific application scenario. The present analysis was conducted with ECG and GSR data collected from 19 different subjects, while boredom was naturally induced during the repetitive playing of a 3D video game. Conventional biosignal features as well as moment-based ones were found to be effective for the automatic recognition of boredom by achieving classification accuracies around 85 percent. Then, the joint use of moments and moment variations with conventional features was found to significantly improve classification accuracy by producing a maximum correct classification ratio of 94.17 percent.

Index Terms—Biosignals, boredom, ECG, emotion recognition, GSR, moments, video games.

1 INTRODUCTION

THE development of machines able to interact with humans in a natural way, close to human-human communication is a key challenge for the years to come. A basic prerequisite toward this goal is the development of advanced computer systems able to understand human affective states [1]. In this line, a large number of research efforts have already been made, trying to recognize emotions from monitored audio-visual [2] and biosignal modalities. Although effective in certain contexts, affect recognition based on audio and visual channels is considered to suffer from several disadvantages when applied in realistic applications [3]. For instance, the visual modality requires that the user's expressions, gestures, etc., are continuously monitored by appropriate camera(s), whereas the audio modality can only work when the user speaks in order to extract features indicative of her/his emotional

state. Furthermore, social masking in this context is an issue of great importance since the audio and visual modalities cannot always reflect the true human emotional state. Automatic emotion recognition (ER) based on biosignals has attracted much attention recently. The Jamesian theory [4] emphasizes the importance of peripheral signals in affect recognition, as it suggests there are specific patterns of physiology that relate to different emotions.

1.1 Related Work

During the last years, several important attempts have been made toward biosignals-based ER [3], [5], [6], [7], underlining the usefulness of peripheral activity for emotion assessment in diverse conditions. Research efforts based on biosignals have so far produced notable results, dealing either with subject-dependent [3], [5], [6], [8] or the more difficult case of subject-independent [6], [7] ER. Within the majority of important previous works, emotions were induced in subjects either by watching video clips [9] or pictures [8], [10], listening to music [6], [11], or recalling good or bad memories [3], [5], [12].

Focusing more on the future applicability of ER systems, virtual reality applications and video games can be considered as extremely fertile fields. Affect recognition applied in VR applications can be used in order to study human behavior during diverse realistic scenarios. An example of this is [13], where biosignals were obtained from car-racing drivers toward the identification of the subject's high stress, low stress, euphoria, and disappointment. The potential development of future game-playing systems which, based on an affective loop [14], will be able to adapt on the basis of the player's emotions also seems very interesting. Such systems will have the capability of identifying whether the player's enjoyment [15], [16] is

- D. Giakoumis is with the Department of Electrical and Computer Engineering, Aristotle University of Thessaloniki, Greece and with the Informatics and Telematics Institute, Centre for Research and Technology Hellas (CERTH/ITI), 6th Km Charilaou-Thermi Road, 57001 (PO Box 361), Thermi-Thessaloniki, Greece. E-mail: dgiakoum@iti.gr.
- D. Tzovaras and K. Moustakas are with the Informatics and Telematics Institute, Centre for Research and Technology Hellas (CERTH/ITI), 6th Km Charilaou-Thermi Road, 57001 (PO Box 361), Thermi-Thessaloniki, Greece. E-mail: {tzovaras, moustak}@iti.gr.
- G. Hassapis is with the Department of Electrical and Computer Engineering, Aristotle University of Thessaloniki, 541224, Thessaloniki, Greece. E-mail: ghass@auth.gr.

Manuscript received 22 Apr. 2010; revised 24 Aug. 2010; accepted 20 Dec. 2010; published online 25 Feb. 2011.

Recommended for acceptance by H. Prendinger.

For information on obtaining reprints of this article, please send e-mail to: taffc@computer.org, and reference IEEECS Log Number TAFFC-2010-04-0027.

Digital Object Identifier no. 10.1109/TAFF-C.2011.4.

reduced and subsequently adapting the playing context accordingly in order to maximize player's involvement and satisfaction. The first step toward this direction is the development of appropriate systems, able to automatically assess the quality of the gaming experience.

The automatic recognition of boredom can be considered of great importance in this context as an emotion that can be investigated complementary to "fun" by game designers [17]. Previous work [18] has already shown that playing simple games like Tetris at different levels of difficulty gives rise to different emotional states that can be defined as boredom, engagement, and anxiety. A 72.5 percent accuracy regarding the identification of boredom with biosignals data derived from 20 subjects was reported. Furthermore, in [19], the affective states of engagement, anxiety, boredom, frustration, and anger were induced in subjects from solving anagrams and playing a variant of the early, classic "Pong" video game. The authors reported an average subject-dependent classification accuracy of 84.23 percent regarding three intensity levels of boredom (low, medium, and high), over data derived from 15 subjects. Following this line and using a 3D video game as the emotion induction stimuli, the present work focuses on the automatic, biosignals-based recognition of boredom during video-game playing.

Biosignals-based ER is based on features extracted from different monitored biosignals, like the Electrocardiogram (ECG) and the Galvanic Skin Response (GSR). These features encode specific characteristics of the monitored signals, known to be connected with emotion-driven changes in the Autonomic Nervous System (ANS) activation. These characteristics, expressed by the extracted features, are then used for the classification of different affective states. Starting from Picard's work about 10 years ago [5], in most biosignals-based ER studies similar sets of features are commonly used for classification purposes. In the rest of this paper, these commonly used features will be referred to as conventional ones. These are common time or frequency-domain statistical features calculated from the monitored biosignals, like the mean, variance, and power of specific frequency bands. Furthermore, since each monitored modality has its own specific emotion-driven responses, several other features are commonly used for each modality, e.g., the Skin Conductance Response (SCR) occurrences [7] of the GSR or the pNN50 [6] of the ECG. Such conventional features are described in Section 2. Although biosignal-based ER has produced good classification accuracies among different emotions, correct classification rates that significantly exceed 90 percent in more-than-two (usually three, four, or more) or even in the more trivial case of two-class classification problems are relatively rare in the literature. Given the complex nature of biosignals, this comes to no surprise; however, it is clear that there is still much room for improvement in the specific domain. In this line, the utilization of novel—in the biosignals domain features, possibly in conjunction with conventional ones, can be expected to further enhance the accuracy of such ER systems.

Different frequency components of ECG (Heart Rate-related) and GSR biosignals have already proven to convey information helpful for automatic ER [6]. The extraction of features with increased frequency discretization capabilities

can thus be thought of as potentially effective in the specific domain. Such features would be able to assess different characteristics of monitored biosignals, related either to their low or higher frequency oscillations. Following this rationale, moments can be expected to prove useful toward biosignals-based ER, as highly discriminative transformations of the input signals, capable of assessing information conveyed through different frequency components. Since Hu introduced the moment invariants [20], orthogonal moments are widely used in pattern recognition, image processing, computer vision, and multiresolution analysis [21]. According to the theory of moments, one or more-dimensional signals can be projected on different polynomials of different orders. These projections then lead to the calculation of the different order moments. When the polynomials used are orthogonal to each other, the different signal projections produce moments with minimum information redundancy. As a result, the different moment orders produced by a signal's moment-based transformation can express different characteristics of the initial signal. Moments are compact representations of the input; most of the information is concentrated in the lower orders. As a result, moments of relatively low orders are usually capable of driving pattern recognition.

Based on the theory of continuous orthogonal polynomials, Legendre and Zernike moments were first introduced by Teague [22]. Orthogonal Legendre and Zernike moments have been successfully applied in image analysis and pattern recognition [23], [24], [25]. Krawtchouk moments were introduced by Yap et al. [26] in an effort to overcome discretization errors caused in numerical approximations of the continuous integrals that are involved in the conventional orthogonal moments kernel functions [27]. Krawtchouk moment-based compact representations have proven to be effective in pattern recognition due to their high discriminative power [28]. They have been successfully applied in image processing [26] and pattern matching for classification purposes over 2D images [29] and 3D objects [28]. Although Legendre and Krawtchouk moments have been proven to be effective in pattern recognition, they have never until now been considered as an option in the field of biosignals-based ER. Therefore, this paper focuses on the potentials of Legendre, Krawtchouk moments and moment variations, toward biosignals-based automatic ER.

1.2 Contribution

Using multisubject data derived from an experiment naturally inducing boredom during video-game playing, this paper initially shows that the automatic recognition of boredom through conventional features extracted from ECG and GSR biosignals is feasible. Then, exploiting the frequency resolution capabilities of moments, the potential of Legendre and Krawtchouk moments applied on biosignals toward ER is for the first time examined. In this context, novel biosignal features based on variations of Legendre and Krawtchouk moments are also proposed. Research in the field of automatic biosignals-based ER is in need of novel and more effective features than the conventional ones commonly used. In this line, the present work proposes for the first time the use of moment-based features in the specific field. It is shown through experimental evaluation that the use of moments (Legendre or

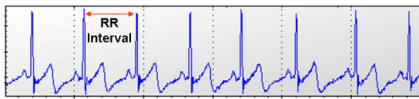


Fig. 1. Typical recorded ECG signal.

Krawtchouk) and the proposed moment variations as biosignal features can improve the classification accuracy of conventional biosignals-based ER systems.

1.3 Paper Outline

In the following, a brief description of the biosignals-based ER framework utilized is provided in Section 2. Section 3 presents the conventional features extracted from the monitored biosignals. Section 4 describes the Legendre and Krawtchouk moments used for feature extraction, along with the proposed moment variations. The LDA-based classifier used is presented in Section 5. Section 6 describes the experimental setup deployed for data collection. Sections 7 and 8 present and discuss the results of this work. Conclusions are drawn in Section 9.

2 BIOSIGNALS-BASED MONITORING FRAMEWORK BACKGROUND

The electrocardiogram is a modality commonly used in order to assess the Heart Rate Variability (HRV). HRV describes the variations between consecutive heartbeats. The regulation mechanisms of HRV originate from the sympathetic and parasympathetic nervous systems and thus HRV can be used as a quantitative marker of the autonomic nervous system's operation [30]. Features extracted from the ECG signal (Fig. 1), reflecting the subject's HRV, have already been used together with features derived from other modalities in a number of studies targeting automatic ER, e.g., [6], [7], [10], [11], [12]. Furthermore, the results of previous studies [18], [19] can be considered as indications that HRV parameters could be useful toward the automatic recognition of boredom.

Most commonly used HRV analysis methods are based on the time and frequency domains [31]. Time-domain HRV parameters are the simplest ones, calculated directly from the RR interval (or InterBeat Intervals—IBI) time series. These are the time series produced from the time intervals between the consecutive “R-peaks” of the raw ECG signal, shown in Fig. 1. The simplest time-domain measures are the mean and standard deviation of the IBIs. Commonly used HRV features are also the RMS of the IBI Sequential Differences (RMSSD) and the percentage within a time period of sequential differences that are over 50 milliseconds (pNN50) [31]. Frequency-domain analysis is commonly based on the calculation of the IBI signal's Power Spectral Density (PSD). The most common frequency-domain HRV features include the powers of VLF (0.003-0.04 Hz), LF (0.04-0.15 Hz), and HF (0.15-0.4 Hz) bands, and the LF to HF ratio [31].

Galvanic Skin Response, also referred to as Electrodermal Activity (EDA), is a measure of skin conductance, which can be seen as an indirect measure of sympathetic nervous system activity [32]. Skin conductance is positively correlated with eccrine gland activity, which is in turn correlated

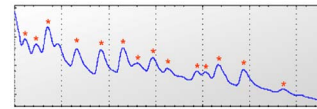


Fig. 2. Typical GSR signal (SCR occurrences marked with asterisks).

with sympathetic nerve activity. There are two main types of EDA fluctuations that occur with stimulation: the momentary phasic responses that occur with stimulation: the momentary phasic responses and the more stable tonic level.

GSR features commonly extracted and used in the literature are the mean level of the GSR signal and the skin conductivity responses (Skin Conductance Response—SCR). SCRs are distinctive short waveforms like the ones indicated by asterisks in Fig. 2. Their occurrence inside a GSR signal signifies ANS activation responses to internal or external stimuli. Both phasic and tonic GSR features are commonly used toward automatic affect recognition [5], [6], [7], [8], [10], [11]. GSR features are considered as a very reliable physiological measure of human arousal [6]. Thus, they can be expected to be useful toward the automatic recognition of boredom, an affective state that can be connected to low levels of arousal. Indeed, in [18] and [19], features extracted from the GSR modality were found to correlate with the subjects self-assessment of boredom.

3 CONVENTIONAL FEATURE EXTRACTION

Various conventional features were extracted from ECG and GSR signals, recorded during trials of the experiment described in Section 6. The calculation of each feature produced a single value per trial, expressing a specific biosignal characteristic. The features used were checked for robustness to potential noise that could appear in the recorded signals given the specific application scenario.

Regarding the ECG modality, HRV-related features were extracted from subject's InterBeat Intervals (IBI) time series. ECG data were collected at a sampling rate of 256 Hz. IBIs were calculated from the subject's recorded Electrocardiogram, directly by the monitoring device's (Procomp5) software. The average (**IBI Mean**) and standard deviation (**IBI SD**) of the IBI signal per trial were extracted as features, along with other typical time-domain and frequency-domain ones, described in Table 1. In order to treat between-subject variations in the recorded ECG signals, all features extracted from the IBI series were normalized by division to their subject-specific baseline values [9], calculated from each subject's baseline measurements, recorded during the Rest session of the experimental process (described in Section 6.3). An exception regarding this normalization was made for pNN50, due to the fact that for some subjects its value during the rest period was zero. This feature was normalized in the span [0, 1] regarding the min and max per trial feature value, calculated for each subject during all of her/his trials.

Regarding the GSR modality, both the tonic and phasic Electrodermal Activity were examined. The features described in Table 2 were extracted from the recorded GSR signals, sampled at the rate of 256 Hz.

Furthermore, following [5], four more features were extracted from both the GSR and IBI signals (Table 3).

TABLE 1
Conventional Features Extracted from the IBI Signal

Name	Description
IBI LF/HF per Trial	The average ratio of the LF band power to the HF band power during a trial: $IBI_{LF/HF} = \left(\frac{\sum_{i=1}^N LFP_i}{\sum_{i=1}^N HFP_i} \right) \quad (1.1)$ where LFP_i and HFP_i are the LF and HF band Powers respectively. Band powers were calculated directly by the monitoring device (Procomp5) software
IBI RMSSD	RMS of the sequential differences of the IBIs per trial: $IBI_{RMSSD} = \sqrt{\frac{1}{N-1} \sum_{i=1}^{N-1} (IBI_{i+1} - IBI_i)^2} \quad (1.2)$ $\forall (IBI_{i+1} - IBI_i) \neq 0$
IBI pNN50	Percentage of the number of sequential IBI differences during a trial that are over 50 ms $IBI_{pNN50} = \frac{nd_{>50}}{nd} \quad (1.3)$ where nd is the total number of sequential IBI differences during the trial, and $nd_{>50}$ is the number of those that are over 50 ms.

All of the above-described features were calculated with data derived from the whole of each trial, apart from those concerning the GSR signal's SCR occurrences, which were calculated over each trial's first 25 seconds. This was due to the fact that the vast majority of recorded trials were about 30 seconds long and uniformity was desired in the period

TABLE 2
Conventional Features Extracted from the GSR Signal

Name	Description
GSR Mean per trial	$gsr_{mean} = \frac{1}{N} \sum_{i=1}^N \bar{G}(i) \quad (2.1)$ where $\bar{G}(i)$ is the normalized GSR signal, calculated similarly to the procedure applied in [33] using: $\bar{G}(i) = (G(i) - G_{min}) / (G_{max} - G_{min}) \quad (2.2)$ where N is the number of GSR samples during the trial, $G(i)$ is a GSR sample, G_{min} and G_{max} are the GSR's min and max values recorded during all the specific subject's game-playing trials
GSR SD per trial	$gsr_{SD} = \sqrt{\frac{1}{N} \sum_{i=1}^N (\bar{G}(i) - \bar{G}_{mean})^2} \quad (2.3)$ where $\bar{G}(i)$ is a sample of the normalized GSR signal, and \bar{G}_{mean} is its average value for the trial.
GSR 1st Derivative Avg and GSR 1st Derivative RMS per trial	Initially, the GSR 1st derivative was calculated: $gsr_d1raw_i = (\bar{G}(i+1) - \bar{G}(i)) / (t_{i+1} - t_i) \quad (2.4)$ where $\bar{G}(i)$ is a normalized GSR sample and t_i is its timestamp. The resulting time-series was convoluted with a smoothing 255-point Bartlett window, similarly to [7], producing signal gsr_d1 . The average and RMS of gsr_d1 were then calculated per trial.
SCRs during a trial	SCR occurrences were identified using gsr_d1 , as described in [7]. From the SCRs and the normalized signal $\bar{G}(i)$, four SCR-based features were extracted for the first 25 seconds of each trial: Number of SCRs , Average Amplitude of SCRs , Average Duration of SCRs and Maximum Amplitude of SCRs

TABLE 3
Conventional Features Extracted Following [5]

Name	Description
$\delta(\text{ibi})$ and $\delta(\text{gsr})$, $\delta_{norm}(\text{ibi})$ and $\delta_{norm}(\text{gsr})$	The mean of the absolute values of the first differences of the raw (3.1) and normalized (3.2) signals: $\delta(x) = \frac{1}{N-1} \sum_{i=1}^{N-1} x_{i+1} - x_i \quad (3.1)$ $\delta_{norm}(x) = \frac{1}{N-1} \sum_{i=1}^{N-1} \bar{x}_{i+1} - \bar{x}_i \quad (3.2)$
$\gamma_{norm}(\text{ibi})$ and $\gamma_{norm}(\text{gsr})$	Similarly, regarding the second differences: $\gamma_{norm}(x) = \frac{1}{N-2} \sum_{i=1}^{N-2} \bar{x}_{i+2} - \bar{x}_i \quad (3.3)$
$f_d(\text{ibi})$ and $f_d(\text{gsr})$	The mean of the convoluted with a Hanning window GSR and IBI signal first differences: $f_d(x) = \frac{1}{N-1} \sum_{i=1}^{N-1} (s_{i+1} - s_i) = \frac{1}{N-1} (s_N - s_1) \quad (3.4)$ where x is the IBI or GSR signal, s_i is the i^{th} sample of the resulting time series of the raw signal, sub-sampled at 16Hz and convoluted with a 3-second Hanning window

In (3.1)-(3.3), x is the IBI or GSR signal and N is the number of signal samples recorded during the trial. As in [5], the normalized signal \bar{x}_i used in (3.2) and (3.3) was calculated by $(x_i - x_{mean}) / x_{sd}$, where x_i is a signal value recorded during a trial, x_{mean} and x_{sd} are the signal's average and standard deviation during the trial, respectively.

over which the specific features were extracted, so as to avoid bias in trials of longer duration. All of the extracted features alterations during a trial were also considered as potential indexes of the subject's boredom. The rationale behind this was that the induction of boredom could possibly have an impact on the way some feature values changed between the first and last seconds of each game-playing trial. Therefore, all features described in this section were also extracted from only the first and last 10 seconds of each trial; then, the ratio between each feature's value calculated from the trial's first 10 seconds to the corresponding value of the last 10 seconds was extracted as an extra feature. These ratios were calculated for all features that were applicable, namely, for all described in this section except the four SCR-related ones and the IBI pNN50. All calculated feature ratios are marked in the remainder of this paper with the extension "FL Ratio."

Concluding, 37 conventional features were extracted in total, 9 from the ECG modality, 12 from the GSR, and further 16 features were calculated as the ratio of each feature between the first and last 10 seconds of each trial.

4 NOVEL MOMENT-BASED BIOSIGNAL FEATURES

Different frequency components of IBI and GSR biosignals have been found to convey information capable of driving automatic ER [6]. This information is commonly assessed through features extracted from the low or band-pass filtered signals. Moments are highly discriminative, compact representations of the input. Lower order moments represent the input's global characteristics and higher orders represent the detail. Different order moments are thus capable of assessing different characteristics of the monitored signals, related to either their low or higher frequency oscillations. Moments can thus be expected to

prove useful toward effective biosignals-based ER. In the following, the Legendre and Krawtchouk moments extracted in this work as biosignal features are described. Furthermore, two novel moment variations are proposed as features potentially useful for automatic ER.

4.1 Legendre Moments

Legendre moments are based on the projection of a signal onto Legendre polynomials, which form a complete orthogonal basis set defined over the interval $[-1, 1]$. For a 1D discrete signal $f(x_i)$, $1 \leq i \leq N$, the 1D Legendre moment of order p [34] is given by

$$L_p = \frac{2p+1}{N-1} \sum_{i=1}^N P_p(x_i) f(x_i), \quad (1)$$

where $x_i = (2i - N - 1)/(N - 1)$ and $P_p(x)$ is the p th order Legendre polynomial given by

$$P_p(x) = \frac{1}{2^p} \sum_{k=0}^{p/2} (-1)^k \frac{(2p-2k)!}{k!(p-k)!(p-2k)!} x^{p-2k}, \quad (2)$$

where x belongs in the span $[-1, 1]$.

In the present work, the following recursive relation [35] was utilized for calculating Legendre polynomials:

$$P_{p+1}(x) = \frac{2p+1}{p+1} x P_p(x) - \frac{p}{p+1} P_{p-1}(x) \quad p \geq 1, \quad (3)$$

with $P_0(x) = 1$ and $P_1(x) = x$.

Legendre moments of orders 0-39 were calculated for the GSR and IBI signals (features **gsr_LgXX** and **ibi_LgXX**, respectively, where XX is the moment order), taken from the first 25 seconds of each trial, so as to ensure uniformity in the extraction process. Given the nature of Legendre polynomials, there could be cases where differences in trial duration could slightly affect the signal characteristics captured from the different moment-based feature orders. Prior to feature extraction, signals were subsampled at 4 Hz and normalized to their subject-specific global min and max values by (2.2). Only the first 40 orders were extracted as features, due to the fact that the use of higher ones would increase complexity and was not expected to provide added value. In fact, after calculating the first 40 Legendre moments of Dirac's delta function and then reconstructing the initial signal [36] with (4) and the first 40 orders, the reconstructed signal's PSD showed that these orders were capable of capturing information conveyed through frequencies approximately up to 0.5 Hz:

$$\hat{f}(x) = \sum_{p=0}^M L_p P_p(x), \quad (4)$$

where M is the highest order used.

4.2 Krawtchouk Moments

Krawtchouk moments are based on a set of orthonormal polynomials, introduced by Mikhail Krawtchouk in 1929. The n -order Krawtchouk classical polynomials [37] are defined in terms of hypergeometric function as

$$K_n(x; p, N) = \sum_{k=0}^N a_{k,n,p} x^k = {}_2F_1 \left(-n, -x; -N; \frac{1}{p} \right), \quad (5)$$

where $x, n = 0, 1 \dots N$, $N > 0$, p belongs in the span $(0, 1)$, ${}_2F_1$ is the hypergeometric function [26]. In order to ensure the numerical stability of the polynomials and achieve orthonormal basis function with unitary weight function, weighted Krawtchouk polynomials were introduced [26]:

$$\bar{K}_n(x; p, N) = K_n(x; p, N) \sqrt{\frac{w(x; p, N)}{r(n; p, N)}}, \quad (6)$$

where $w(x; p, N)$ and $r(n; p, N)$ are defined as

$$w(x; p, N) = \binom{N}{x} p^x (1-p)^{N-x}, \quad (7)$$

$$r(n; p, N) = (-1)^n \left(\frac{1-p}{p} \right)^n \frac{n!}{(-N)_n}. \quad (8)$$

In this work, the following recurrent relations [37] were used so as to reduce the high computational complexity of weighted Krawtchouk polynomials calculation:

$$K_{n+1}(x; p, N) = \left(1 + \frac{n-np-x}{pN-pn} \right) K_n(x; p, N) - \frac{n-np}{pN-pn} K_{n-1}(x; p, N), \quad (9)$$

$$w(x+1; p, N) = \frac{w(x; p, N) p(N-x)}{x+1-p-xp}. \quad (10)$$

The initial conditions for (9) and (10) are: $K_0(x; p, N) = 1$, $K_1(x; p, N) = 1 - (1/(Np))x$, and $w(0; p, N) = (1-p)^N$.

For a 1D signal $f(x_i)$ of length N , the weighted Krawtchouk moments \bar{Q}_n [38] are defined as

$$\bar{Q}_n = \sum_{i=1}^N \bar{K}_n(i-1; p, N-1) f(x_i), \quad (11)$$

where $x_i = i - 1$.

In this study, the 40 first Krawtchouk moments (0-39) were calculated with (11) for the GSR and IBI time series (features **gsr_KrXX** and **ibi_KrXX**, respectively, where XX is the moment order), by taking into account the whole N samples corresponding to the first 25 seconds of each trial's signal. Prior to Krawtchouk-based feature extraction, GSR and IBI signals were subsampled at 4 Hz and normalized to their subject-specific global min and max values by (2.2). In all cases the parameter p was taken equal to 0.5 in order for the region-of-interest of the feature extraction process to be centered at the half of each trial's first N samples. The analysis was restricted to the first 40 moment orders, following the same rationale as in the Legendre case; (12) was used [38] for the reconstruction of the delta function using Krawtchouk moments, and the reconstructed signal's PSD showed that the first 40 orders were capable of capturing information conveyed through frequencies approximately up to 0.8 Hz:

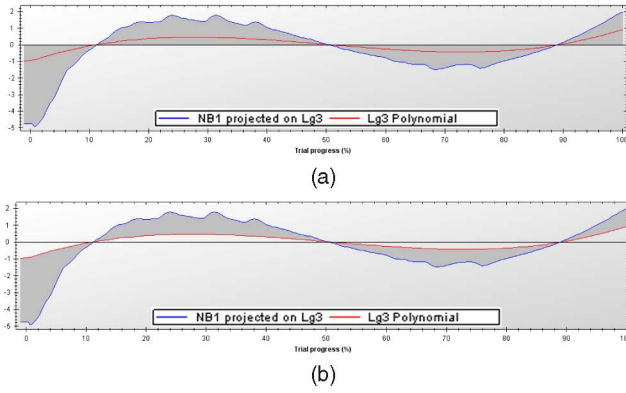


Fig. 3. Legendre third order polynomial and the projected (NB1) GSR signal, using $(2p+1)^*P_p(x_i)^*f(x_i)$. (a) Area utilized from (1), marked with dark gray. (b) Area utilized from (17), marked with dark gray.

$$\hat{f}(x) = \sum_{n=0}^M \bar{Q}_n \bar{K}_n(x; l, N-1), \quad (12)$$

where M is the highest order used.

4.3 Variations of Legendre and Krawtchouk Moments

The analysis presented in Section 7.1 indicates that moment-based features could possibly enhance classification accuracy of biosignals-based ER systems. Following this rationale, novel biosignal features based on the theory of moments could also prove helpful in this field. Motivated by this, variations of the original Legendre and Krawtchouk moments were also extracted as features and their effectiveness was experimentally examined (as described in Section 7) in the specific application scenario.

As shown from (1) and (11), the calculation of Legendre and Krawtchouk moments takes into account the area contained between the initial signal projected on the Legendre or Krawtchouk polynomials, respectively, and the x -axis (marked in the Legendre-based example of Fig. 3a with dark gray). Instead of utilizing this whole area, the proposed variations are based on the area between the signal projection and the specific order polynomial, marked with dark gray in Fig. 3b.

Thus, using (13) and (14) instead of (1) and (11), respectively, Legendre and Krawtchouk-based variations were extracted as further potentially useful features from each of the ECG and GSR modalities:

$$L_p^{\text{mod}} = (2p+1) \sum_{i=1}^N P_p(x_i)(f(x_i) - 1), \quad (13)$$

$$\bar{Q}_n^{\text{mod}} = \sum_{i=1}^N \bar{K}_n(i-1; p, N-1)(f(x_i) - 1). \quad (14)$$

The idea behind these novel features was to suppress the static parameter of the original moments calculation, namely the area between the projection polynomial and the x -axis, which is always identical. Thus, although the signal is again transformed on the basis of Legendre and Krawtchouk polynomials, the transformation product now contains less information that is identical among all cases of different input signals.

The main feature of (13) and (14) is the subtraction of the original (Legendre or Krawtchouk, respectively) polynomial from the projected signal. Taking as an example the modified Legendre moments, it can be shown that (13) results to the original moment order, after the subtraction of the same order calculated for the unit function ($f(x_i) = 1, \forall x_i > 0$) and suppression of the $N-1$ normalization factor:

$$L_p^{\text{mod}} = (N-1) \left\{ \left(\frac{2p+1}{N-1} \right) \sum_{i=1}^N P_p(x_i) f(x_i) - \left(\frac{2p+1}{N-1} \right) \sum_{i=1}^N P_p(x_i) \right\}. \quad (15)$$

The term $\left(\frac{2p+1}{N-1} \right) \sum_{i=1}^N P_p(x_i) f(x_i)$ of (15) is identical to (1), which stands for the original moment, calculated for the signal $f(x_i)$. The term $\left(\frac{2p+1}{N-1} \right) \sum_{i=1}^N P_p(x_i)$, subtracted in (15) from the original moment, stands for the moment calculation of the unit function ($f(x_i) = 1, \forall x_i > 0$). Furthermore, in the proposed Legendre moment variation, the result is multiplied by $N-1$ so as to suppress the $N-1$ normalization factor employed in the original moment calculation.

As a result, the new transformations are still capable of assessing signal information conveyed through different frequency components (related to the different polynomial orders), but at the same time, can be considered as even more indicative of the input signal's characteristics.

Summarizing, based on the first 40 Legendre polynomials, 40 features were extracted from each of the GSR and IBI signals (features `gsr_LgmodXX` and `ibi_LgmodXX`, respectively, where `XX` is the order of the polynomial used), by following the same procedure described in Section 4.1 and using (13) instead of (1). Similarly, on the basis of the first 40 Krawtchouk polynomials, 40 further features were extracted from each signal (features `gsr_KrmodXX`, `ibi_KrmodXX`), by using (14) instead of (11).

5 LDA-BASED CLASSIFIER

Linear Discriminant Analysis (LDA) is a method for finding the linear combination of features that best separates available data into two or more classes. The resulting combination is commonly used for dimensionality reduction, but can be used as a linear classifier as well. In this study, a linear classifier was preferred instead of a nonlinear one, due to the fact that the former are less computationally expensive to train and, moreover, they are based on simpler, linear models and thus can be expected to generalize better in new databases. Using a more sophisticated nonlinear classifier could possibly provide better results for some feature sets, but these results could have been biased by the fact that a superior classifier was used, capable of better adjusting its model to the specific given data set. LDA-based classifiers have proven effective in the field of biosignals-based ER [3], [6]; in [3], LDA was even found to work better than the nonlinear QDA.

In Fisher's LDA, the optimum projection for a given data set is realized through the transformation matrix \mathbf{W} , which is calculated so as to maximize the formula:

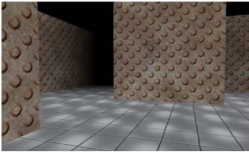


Fig. 4. Screenshot of the 3D Labyrinth game.

$$J(\mathbf{W}) = \frac{\mathbf{W}^T \cdot \mathbf{S}_b \cdot \mathbf{W}}{\mathbf{W}^T \cdot \mathbf{S}_w \cdot \mathbf{W}}, \quad (16)$$

where \mathbf{S}_b is the “between class scatter matrix” and \mathbf{S}_w is the “within class scatter matrix” of the train data set [6].

The classifier used in this work was based on a two-class Fisher LDA classification schema. In two-class LDA, data from the initial feature space is projected on a single projection axis which best discriminates training data among the available classes. Thus, once the optimum transformation vector \mathbf{W} is calculated from the train data set, it can be used to calculate the projection of each class Centroid and each new (test) case to the transformation axis. Classification can then be performed in the transformed space by assigning the new case to its less distant class found over the projection axis using:

$$\min((\mathbf{F}(case)\mathbf{W}^T - \mathbf{m}_0\mathbf{W}^T), (\mathbf{F}(case)\mathbf{W}^T - \mathbf{m}_1\mathbf{W}^T)), \quad (17)$$

where $\mathbf{F}(case)$ is the feature vector of the test case, m_0 and m_1 are the centroids of the two classes under consideration calculated using the training data, and \mathbf{W} is the transformation matrix calculated from (16).

Leave-one-out cross validation (LOOCV) was employed [5], [6], [19]; the final Correct Classification Ratio (CCR) of the classifier was calculated by $CCR = N_c/N$, where N_c is the number of cases correctly classified and N is the total number of cases constituting the full data set.

6 EXPERIMENTAL SETUP

In order to collect data appropriate for the purposes of this study, an experiment was conducted with the aim to monitor the subject’s biosignals while the state of boredom would be naturally induced from the repetitive playing of the same 3D Labyrinth game. Each repetition was regarded as a single trial during which the subject tried to find the Labyrinth’s exit. The subject’s actual affective state during the experimental session was assessed with the use of questionnaires, filled in after each trial.

6.1 Stimuli

A basic 3D Labyrinth game (Fig. 4) was developed for the purpose of the experiment. In order to complete the game, players had to simply find the exit. The player could walk through the mazy corridors of the labyrinth using a 3D first person camera which was controlled by the WASD/Arrow keys and the mouse, a standard method used in commercial games. The game was developed in C++ using “OGRE” for graphics and the “Bullet” physics library for physics simulation.

In order to effectively induce boredom due to loss of interest, the Labyrinth was designed to be a very simple one. Furthermore, in all repetitions the player started from the same point and the Labyrinth exit was always at the

same place. As a result, usually after the third or fourth trial the subject had learned the shortest path to the exit. Thus, even though, in the beginning (first 2 or 3 trials), the game was kind of exciting, as soon as the subject had learned the shortest path to the exit, the stimuli became an absolutely repetitive HCI task, ideal to induce negative emotions like boredom due to loss of interest.

A widely accepted component process model of emotion is Scherer’s [39], [40] sequence of five “stimulus evaluation checks” (SECs), which describe the eliciting and differentiating mechanisms in emotion arousal. In particular, according to the appraisal theory an individual is assumed to evaluate situations and events in terms of

1. their novelty,
2. their intrinsic pleasantness,
3. their conduciveness to satisfying major needs and goals,
4. the individual’s coping potential (control, power, adjustment capacity), and
5. the self and norm compatibility of the event encountered.

From the appraisal theory point of view, novelty was the main factor manipulated during the experimental session. According to the appraisal theory, very low novelty is a key factor for boredom induction. Furthermore, low novelty may result in the induction of further emotions, such as irritation/cold anger. Frustration was a factor also monitored by self-reports throughout the experiment; however, the specific study focuses on the automatic recognition of boredom induced during the specific repetitive video-game playing task.

The emotion induction stimuli of this study was decided to be a game that relates to current commercial games played by vast amounts of gamers and at the same time was capable of inducing boredom. For this purpose, the Labyrinth game was based on state-of-art 3D graphics, with a gameplay basis closely related to modern, massively played 3D first person RPGs. Considering Malone’s [41] widely adopted principles of intrinsic qualitative factors for engaging game play, namely, challenge, curiosity, and fantasy, the stimuli used in this study (especially after the first or second trial) was designed in an effort to be lacking in all three of them. In addition to the fact that novelty was at a very low level, this made the stimuli an ideal process to effectively induce boredom. In fact, during the experiments there were two subjects who, according to their self-assessment, did not feel “not bored” at any stage of the whole session.

Further generalizing the protocol to current commercial games, we could consider the case of such a game which does not automatically increase its difficulty level as time goes by and a situation where the player is forced to play the same, very easy level of the game repeatedly. Whatever the game, it is almost sure that in this case there will be a point where the player will get bored and lose interest in it. The point at which game difficulty increases and new challenges are posed to the player could, in the future, be manipulated by appropriate machines which will be able to assess a player’s enjoyment and understand whether the player is starting to get bored so as to adjust the gaming

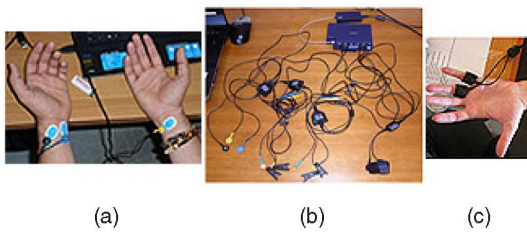


Fig. 5. Experimental setup: (a) ECG sensors, (b) the Biosignals Monitoring Device, and (c) GSR sensors.

context accordingly. A basic prerequisite for this can be considered the development of appropriate systems, capable of effectively detecting boredom, a goal toward which the present study works.

6.2 Hardware Setup

Both ECG and GSR signals were recorded using a Procomp5 Infiniti device (Fig. 5b). One three-electrode ECG sensor was placed on the subject's forearms (Fig. 5a) or, in cases of very low cardiac pressure, on her/his chest. Although differences in the ECG signal may exist between chest or limb wrist-based ECG recordings, effective R-peak detection and subsequent extraction of the IBI time series was equally efficient from both of these ECG recording types in the specific work's context. Autoadhesive Ag/AgCl bipolar surface electrodes (bandwidth 10-500 Hz, pickup surface 0.8 cm², interelectrode distance 2 cm) were used for the ECG signal acquisition. Furthermore, one two-electrode GSR sensor was placed on the subject's left-hand ring and small fingers (Fig. 5c). This GSR sensor setup was chosen so as to be less obtrusive for subjects during handling the keyboard input game device. The synchronization of measurements and the game was based on the Network Time Protocol (NTP).

6.3 Participants and Procedure

The experiment was performed with 19 subjects, 14 males and 5 females, who frequently used computers in their work. Participants were between 23 and 44 years old with 48 percent of them being 25 and 26. Initially, subjects were asked to sign a consent form. After that, the sensors were installed while the subject answered questions regarding personal details (age, etc.) in the prequestionnaire. At this point, the proper sensor placement was ensured by carefully checking the robustness of signal delivered from each monitoring modality. The recorded signals were checked online for artifacts due to external noise or mechanical causes (e.g., subject's motion). The preparation was renewed when severe artifacts were observed. Due to the nature of the experiment, no severe artifacts were expected to appear during sessions. However, in order to further ensure that recorded signals did not contain artifacts severe enough to the extent that the extracted features calculation could have been spoiled, some of the monitoring device software's capabilities for noise removal were utilized during the data processing phase, such as notch filtering at 50 Hz (to cater to possible noise induced from the electrical power supply) or compensation in the IBI signal for badly detected R-peaks.

Once the sensors were properly placed, the subject was asked to relax for one minute in order for the signals to

stabilize and calibration data to be recorded, during the experiment's Rest session. After the end of the Rest period, the 3D Labyrinth game was presented to the subject and, from this point, s/he would play the game repeatedly. Each experimental session was constituted of at least 10 trials. Each trial started when the subject started playing the Labyrinth game and stopped as soon as s/he had found the exit or a 10 minute time-limit had expired. Trials usually lasted from one-half to 8 minutes, with the majority of them lasting around half a minute. A mid-trial relaxation period of one minute was assigned between each trial. During this period, subjects filled in the mid-trials questionnaire, where they had to answer a few Likert-scaled questions, including one for the self-assessment of boredom. The latter asked subjects directly whether they were feeling bored during the last trial. Participants had to answer this question using a scale in the range [1, 5], labeled as "Not at all"- "Very much." It has to be noted that although the between-trial recovery period of one minute utilized could be considered as relatively short, its duration was selected as such in order to provide the best trade-off possible between further boring participants with reoccurring long recovery periods versus allowing the participants bodies enough time to adequately recover from the previous trial. Given the fact that trials usually lasted for about 30 seconds, longer reoccurring recovery periods could have had the effect of inducing even more boredom on participants than the game itself. Preliminary tests showed that the 1 min recovery period allowed for participants' bodies to adequately recover given the specific application scenario, and also allowed for the repetitive game playing to be kept as the main factor of boredom induction.

Although the aim of each session was to induce boredom, participants were not informed prior to or during the experiment about this fact. They were only told that they would play the 3D Labyrinth game repeatedly while their biosignals would be monitored, with no further explanations regarding the overall experiment's target. Furthermore, questionnaires were written in such a way that they would not hint at the fact that participants should get bored during the experiment. For this purpose, the question of self-assessment of boredom was placed within a set of questions assessing other parameters, like the subject's frustration, flow, and immersion. By keeping the experiment's target hidden from participants, it was ensured that, during the session, boredom would be induced as naturally as possible through video-game playing, and the induction process would not be influenced by the subject's prior knowledge of the fact that s/he "should" get bored. The experiment continued until subjects had played a minimum of 10 trials and had signaled boredom in the mid-trial questionnaire at least two times in a row, by answering "5" at the respective question.

6.4 Data Annotation

The initial data set consisted of 221 trials from 19 subjects playing the 3D Labyrinth game. During data annotation, trials were labeled as "bored" and "not bored" ones. Labeling was based on the subject's answers to the boredom self-assessment question. Thus, trials after which subjects answered "1" or "2" were labeled as "not bored" and trials after which subjects answered "4" or "5" were labeled as "bored" ones. Thirty-two trials after which the answer

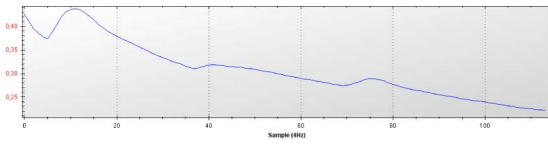


Fig. 6. GSR signal recorded during a “bored” trial (B1).

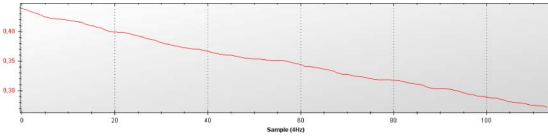


Fig. 7. GSR signal recorded during a “bored” trial (B2).

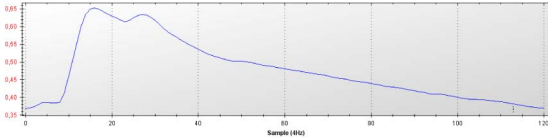


Fig. 8. GSR signal recorded during a “bored” trial (B3).

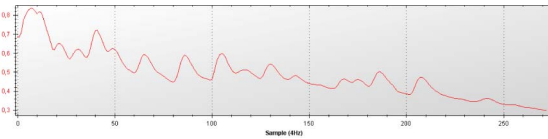


Fig. 9. GSR signal recorded during a “not bored” trial (NB1).

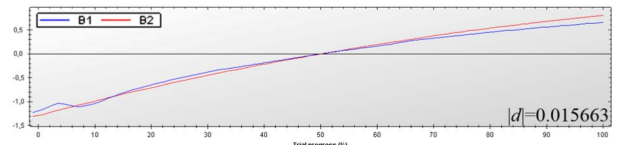
was “3” were excluded from further analysis. The final data set obtained after this procedure consisted of 189 trials, 60 “not bored” and 129 “bored” ones.

7 RESULTS

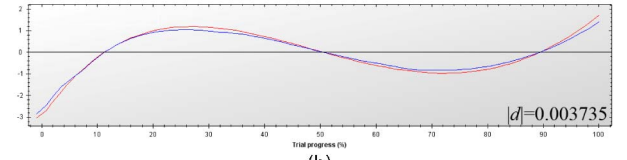
7.1 Analysis on the Comparative Performance of Moment-Based Biosignal Features

The Legendre-based transformation of the GSR signal which leads to the calculation of Legendre moments is demonstrated in the following. For this purpose, characteristic trials annotated as “bored” and “not bored” ones are taken as examples which were recorded during the experiment described in Section 6. Figs. 6, 7, and 8 present the GSR signal recorded during three “bored” trials (B1, B2, and B3, respectively), taken from three different subjects. Fig. 9 presents the GSR signal recorded during a “not bored” trial (NB1). Signals B1 and NB1 were recorded from the same subject.

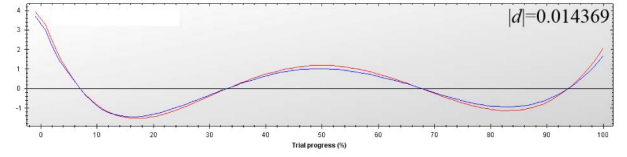
Fig. 10 compares the Legendre-based transformation of signals B1 and B2, whereas Fig. 11 compares the corresponding transformations of B1 and NB1. The signals are projected on Legendre polynomials of the first three orders selected after Sequential Backward Search was applied at the F_Set_CLL initial feature set as described in Section 7.5. These projections are based on the projection formula used in (1). It is clear that the projection of B1 and B2 over these three low order Legendre polynomials tends to produce a similar result. Moreover, the transformed B1 and NB1 signals appear significantly different to each other than B1 and B2 do. The absolute differences $|d|$, shown in Figs. 10 and 11, between the specific order moments calculated for these characteristic trial signals indicate that in these given



(a)

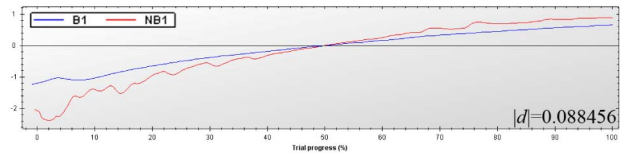


(b)

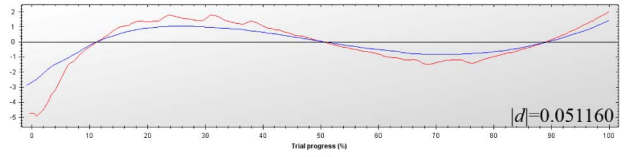


(c)

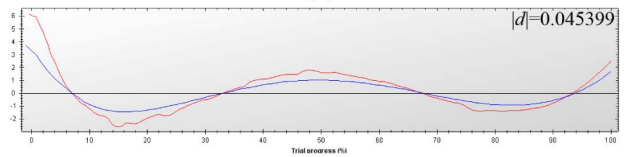
Fig. 10. B1 and B2 GSR signals projected on Legendre polynomials of different orders with the term $(2p + 1) * P_p(x_i) * f(x_i)$ of (1). $|d| = |L_p(B1) - L_p(B2)|$ is the absolute difference of the specific order moments of the two signals, B1 and B2. (a) Order 1. (b) Order 3. (c) Order 4.



(a)



(b)



(c)

Fig. 11. B1 and NB1 GSR signals projected on Legendre polynomials of different orders with the term $(2p + 1) * P_p(x_i) * f(x_i)$ of (1). $|d| = |L_p(B1) - L_p(NB1)|$ is the absolute difference of the specific order moments of the two signals, B1 and NB1. (a) Order 1. (b) Order 3. (c) Order 4.

cases, Legendre moments produce larger differences between “bored” and “not bored” trials than between different “bored” ones. On the contrary, for the same signals, conventional GSR features (selected after SBS applied at the initial conventional data set F_Set_C , as described in Section 7.3), such as $f_d(\text{gsr})$ and $\delta_{\text{norm}}(\text{gsr})$ **FL Ratio**, were found to produce higher $|d|$ values for the case of B1 and B2 comparison (0,00065 and 0,246934332, respectively) than for the comparison of B1 and NB1 (0,00017 and 0,224628032, respectively). Signal B1 was thus found from these features to be more similar to NB1 than to B2. Although the specific conventional features were selected among the best “conventional features only” set,

TABLE 4
Feature Differences between B3, B1, and NB1

Conventional Feature	B3 - B1	B3 - NB1	Legendre Moment	B3 - B1	B3 - NB1
GSR Mean	0.16977	0.0109	1	0.0039	0.0846
GSR SD	0.1698	0.0147	3	0.1084	0.1596
GSR 1st Derivative RMS	0.1078	0.0084	4	0.0887	0.1341
SCRs Average Amplitude	0.4645	0.2839	5	0.0248	0.0514

as explained in the following they can be considered as ineffective toward classifying boredom among these three given trials. However, the Legendre-based transformations appear to work well in the specific cases.

A further comparison between the GSR signal of another bored trial (B3, shown in Fig. 8) against B1 and NB1 indicates one more case where Legendre moments prove helpful for the effective recognition of boredom (Table 4). In this case, the majority of conventional features selected from SBS over the F_Set_C initial feature set find B3 more similar to NB1 than to B1. However, for the specific cases, all of the first four Legendre moments selected again correctly indicate that B3 is more similar to B1 than to NB1.

Taking as an example of the GSR modality, Legendre moments were found in this brief analysis capable of providing biosignal transformations of substantial discrimination potential between the “bored” and “not bored” states. It can be similarly shown that Krawtchouk moments are also capable of providing such useful transformations as well. Moments can thus be expected to have a promising potential toward solving the classification problem addressed in this work, namely, the automatic, biosignals-based recognition of boredom, either by replacing conventional features or by being jointly used with them.

The above analysis was based on a few trials in order to demonstrate the mechanism on the basis of which moment-based features can enhance classification accuracy in this work. In an effort to generalize to further trials and subjects, one-way ANOVA tests were conducted over all extracted features (conventional and moment-based ones) and the full database, trying to further identify whether the features were capable to differentiate well between all bored and not bored trials recorded from all the participants. The analysis was conducted over all conventional features, the Legendre (40 GSR and 40 IBI) and Krawtchouk (40 GSR and 40 IBI) ones, as well as over the Legendre (40 GSR and 40 IBI) and Krawtchouk (40 GSR and 40 IBI) moment variations presented in Section 4.3. The ANOVA results illustrated that only 10 (8 GSR and 2 IBI) out of the 37 (27.02 percent) conventional features showed significant differences ($p < 0.05$) between bored and not bored trial classes. On the other hand, a large percentage of the moment-based features showed significant difference between the two trial classes; 118 out of the total 160 (73.75 percent) moment-based GSR features extracted and 71 out of the total 160 (44.38 percent) IBI moment-based ones showed significant ($p < 0.05$) difference. Furthermore, 8 (21.62 percent) conventional (6 GSR and 2 IBI), 87 (54.38 percent) GSR and 44

TABLE 5
Confusion Matrix for the Best Conventional Feature Set
 $CCR(F_Set_C) = 85.19\%$

	Classified as Not Bored	Classified as Bored	total	class CCR
Not Bored (NB)	51	9	60	85%
Bored (B)	19	110	129	85.3%

(27.5 percent) IBI moment-based features showed significant differences at the $p < 0.01$ level. From the above, it can be concluded that a large number of moment-based features were found to have good potential to prove effective toward automatic boredom recognition on the basis of the classification schema used in this work.

7.2 Feature Selection

Since a large number of features were calculated for the purposes of this study, it was necessary to employ a feature selection technique in order to remove features with low discriminative power in the differentiation between the “bored” and “not bored” player state, resulting in the best classification accuracy. Thus, for selecting the most appropriate features, Sequential Backward Search (SBS) was employed, in combination with the LDA-based classifier described in Section 5. Several other feature selection approaches have been proposed in the literature [42], like Sequential Forward Search, Genetic Algorithm, etc.; however, SBS was selected in this work, similarly to [6]. By starting with a full, initial feature set, SBS initially calculates a criterion value. In our case, the criterion value was the CCR of the LDA-based classifier after LOOCV. An iterative feature removal process is then employed; on each iteration, the feature whose removal increases more the criterion value is definitely removed from the feature set. As a result, the features that produce the best CCR are finally selected from the initial feature set.

It has to be noted that in general, training of automatic classification systems requires special attention so as to avoid overfitting effects. In our case, feature selection was done on the basis of LOOCV, following the rationale behind the procedure applied in [6] and other relevant studies. Feature selection was thus done only on the training set so as to avoid the selection of overfitting features.

SBS was applied in several initial sets, consisting either of conventional GSR and ECG features only, Legendre or Krawtchouk moments, and moment variations extracted as features from the GSR and IBI signals, as well as combinations of them, all described in the following.

7.3 Classification with Conventional Features

SBS was initially applied to feature set F_Set_C , consisting of the 37 conventional features only. A final feature set of 14 features (GSR Mean, GSR 1st Deriv RMS, Number of SCRs, $f_d(\text{gsr})$, Average Amplitude of SCRs, GSR SD, $\delta_{\text{norm}}(\text{gsr})$ FL Ratio, IBI SD, IBI RMSSD, $\gamma_{\text{norm}}(\text{ibi})$, IBI LF/HF FL Ratio, IBI RMSSD FL Ratio, $\delta(\text{ibi})$ FL Ratio, $\gamma_{\text{norm}}(\text{ibi})$ FL Ratio) was selected, producing an average CCR of 85.19 percent, by classifying 161 out of the total 189 cases correctly. Table 5 shows the confusion matrix; its

TABLE 6
CCRs Obtained from SBS Applied on Each of the Moment-Based Transformations of the GSR and IBI Signals Separately

Initial feature set	CCRS OBTAINED AFTER SBS	
	GSR features only	IBI features only
Conventional	77.25%	75.66%
Lg ₀₀ – Lg ₃₉	78.84%	77.25%
Kr ₀₀ – Kr ₃₉	78.31%	75.13%
Lg _{mod00} - Lg _{mod39}	80.95%	79.37%
Kr _{mod00} - Kr _{mod39}	82.11%	75.13%

last column provides the CCR obtained for each class (Not Bored-Bored) separately.

7.4 Classification Using Only Moments and Their Variations

Bearing in mind that different moment-based transformations could prove more effective for one signal type in biosignals-based ER, SBS was initially applied to 10 different initial feature sets, consisting of the conventional, Lg, Kr, Lg_{mod}, and Kr_{mod} features, extracted from the GSR and IBI signals separately. This was done in order to compare moment-based transformations with conventional features with respect to each monitored modality and to identify the most useful moment-based transformation per signal type for the specific classification problem.

As shown in Table 6, the most effective transformation regarding the GSR modality was found to be Kr_{mod} since, after applying SBS on only the GSR Kr_{mod} features, a CCR of 82.11 percent was achieved. Furthermore, the most effective transformation of the IBI time series was found to be Lg_{mod}; SBS produced in this case a CCR of 79.37 percent.

The joint use of moment-based features extracted from both the GSR and IBI signals was then examined (Table 7). Following the results of Table 6, initially the combination of the 40 Kr_{mod} GSR features, together with the 40 Lg_{mod} IBI ones was used as initial feature set (F_Set_K_{mod}L_{mod}) for SBS, which produced a max average CCR of 86.77 percent (class CCR: NB: 75 percent, B: 92.3 percent), after selecting 22 gsr_Kr_{mod}XX (XX = 2, 3, 9, 10, 12-17, 19-21, 24, 27-29, 31-34, 37) and 15 ibi_Lg_{mod}XX (XX = 0, 2, 5, 9, 13, 21, 23, 26-28, 31, 32, 35, 36, 38) features. As shown

TABLE 7
CCRs from SBS Applied on Different “Moment-Based Only” Sets

Initial feature set	CCR AFTER SBS
F_Set_K _{mod} L _{mod}	86.77% (164/189)
F_Set_KL	84.66% (160/189)
F_Set_K _{mod} K _{mod}	84.66% (160/189)
F_Set_L _{mod} L _{mod}	83.07% (157/189)
F_Set_LL	79.37% (150/189)
F_Set_KK	74.6% (141/189)

TABLE 8
CCRs from SBS on Different Initial Sets of Moment-Based Features Combined with the Conventional Ones Class Prior Probabilities: NB = 31.75%, B = 68.25%

Initial feature set	CCR AFTER SBS	CCR(NB)	CCR(B)
F_Set_CK _{mod} L _{mod}	94.71% (179/189)	88.3%	97.7%
F_Set_CLL	92.59% (175/189)	88.3%	94.6%
F_Set_CKK	92.06% (174/189)	83.33%	96.12%
F_Set_CKL	92.06% (174/189)	86.67%	94.57%
F_Set_CK _{mod} K _{mod}	91.01% (172/189)	85%	93.8%
F_Set_CL _{mod} L _{mod}	89.95% (170/189)	81.67%	93.8%

The names of these initial feature sets are in accordance to the names of the ones presented in Table 7.

in Table 7, this was the initial feature set among the “moment-based only” ones that produced the best result. Furthermore, it has to be noted that, using this set, three more cases were correctly classified, in total, than when conventional features were only used, resulting in an increase of 1.58 percent in the best CCR.

As also shown in Table 7, by further applying SBS to the F_Set_L_{mod}L_{mod} set consisting of all of the Lg_{mod} GSR and IBI features, a maximum CCR of 83.07 percent was achieved. Also, SBS applied on the F_Set_K_{mod}K_{mod} set, consisting of the 80 Kr_{mod} GSR and IBI features, produced an 84.66 percent CCR.

Furthermore, using the original moments, SBS was applied on a set that consisted of the 40 GSR and the 40 IBI Legendre moments (F_Set_LL), resulting in a max 79.37 percent CCR. Similarly, using only the Krawtchouk GSR and IBI moments (F_Set_KK set), SBS achieved a CCR of 74.60 percent. Finally, as shown in Table 6, the difference between the max CCRs obtained from the Legendre and Krawtchouk GSR moments was relatively low; one more case was misclassified with Krawtchouk GSR features. Thus, further to F_Set_LL, the Krawtchouk GSR moments together with the Legendre IBI ones were also fed to the SBS (F_Set_KL); a CCR of 84.66 percent was then produced.

7.5 Classification with Conventional Features and Moments

SBS was then applied to initial feature sets consisting of the combinations of GSR and IBI conventional features and moment-based GSR and IBI ones. As shown in Table 8, all feature combinations used as initial “moment-based only” feature sets (Table 7) were fed to the SBS together with the conventional GSR and IBI features. Apart from the total CCRs obtained for the whole data set, Table 8 provides also the CCRs obtained per class; not bored—CCR(NB) and bored—CCR(B) separately.

Following the good classification results obtained when GSR Kr_{mod} and IBI Lg_{mod} features were used alone as initial feature sets, SBS was applied to their combination with the conventional features (F_Set_CK_{mod}L_{mod}). As a result, SBS selected 50 features (GSR 1st Deriv RMS, $\delta_{norm}(gsr)$, Average Amplitude of SCRs, $\delta_{norm}(gsr)$ FL Ratio, f_d (gsr) FL Ratio, gsr_Kr_{mod}XX:XX = 4, 7, 8, 12-17, 19, 21, 23, 24, 26, 28, 30, 31, 33, 34, 36-39, IBI Mean, IBI RMSSD, IBI Mean FL Ratio, IBI SD FL Ratio, IBI LF/HF FL Ratio, IBI RMSSD FL Ratio, and ibi_Lg_{mod}XX:XX = 0-2, 5, 6, 9, 13, 15, 19, 20,

TABLE 9
Confusion Matrix after SBS
over $F_Set_CK_{mod}L_{mod}$, $CCR = 94.71\%$

	Classified as NB	Classified as B	total	CLASS CCR
NB	53	7	60	88.3%
B	3	126	129	97.7%

22, 23, 29-31, 36, 38), achieving a max average CCR of 94.71 percent (Table 9).

Furthermore, using F_Set_CLL as the initial feature set, consisting of the conventional GSR and IBI features together with the GSR and IBI Legendre moments, SBS achieved a max average CCR of 92.59 percent (Table 8). When all conventional features and all Krawtchouk moments were used (F_Set_CKK), SBS achieved a CCR of 92.06 percent, similarly to F_Set_CKL . SBS was also applied to other combinations ($F_Set_CL_{mod}L_{mod}$, $F_Set_CK_{mod}K_{mod}$), however none of them produced better results than the $F_Set_CK_{mod}L_{mod}$ and F_Set_CLL sets (Table 8).

7.6 Leave-One-Subject Out Cross Validation

In order to examine how the results obtained generalize to cases of unseen participants, the best feature sets selected from LOOCV were evaluated over their discriminative ability using leave-one-subject-out cross validation (LOSOVC) as well. During this process, the classifier was trained with all cases but the ones which belonged to the subject from which test cases were taken.

Table 10 summarizes the CCRs obtained with the best features selected from the conventional feature set (F_Set_C), and the ones achieved with the conventional and moment-based feature combinations. From Table 10, it is clear that also in LOSOCV, the combination of conventional features with moment-based ones again enhanced classification accuracy. The best CCR was once more obtained from the $F_Set_CK_{mod}L_{mod}$ feature set.

8 DISCUSSION

The classification results presented in Table 5 provide first of all a strong indication that boredom can be assessed up to a satisfying extent with the use of conventional features extracted from ECG and GSR biosignals, like the ones selected from SBS over this study's F_Set_C feature set. Then, a comparison between Tables 5 and 7 shows that when Krawtchouk, Legendre moments, or their proposed variations were used as features instead of conventional ones, CCRs close to the "conventional features" case were achieved. In fact, using the proposed Kr_{mod} GSR and Lg_{mod} IBI features instead of conventional ones even slightly increased classification accuracy in the given data set.

This comes in accordance to the results presented in Table 6, where it is shown that the suppression of the "static parameter" from the calculation of Legendre and Krawtchouk moments (as explained in Section 4.3) produced highly effective biosignal features in the given ER application scenario. The proposed Kr_{mod} features and Lg_{mod} ones were found as the most effective for the GSR and IBI modalities, respectively, in the given data set.

Focusing on the joint use of conventional features with moment-based ones, by comparing Table 5 with 10, it is

TABLE 10
CCRs from SBS on Different Initial Sets of Moment-Based Features Combined with the Conventional Ones (LOSOVC)

Initial feature set	CCR AFTER SBS	CCR(NB)	CCR(B)
$F_Set_CK_{mod}L_{mod}$	89.42% (169/189)	83.3%	92.25%
$F_Set_CK_{mod}K_{mod}$	85.19% (161/189)	83.3%	86.05%
F_Set_CLL	83.07% (157/189)	88.3%	80.6%
F_Set_CKK	83.07% (157/189)	85%	82.17%
F_Set_CKL	82.01% (155/189)	85%	80.62%
$F_Set_CL_{mod}L_{mod}$	80.42% (152/189)	80%	80.62%
F_Set_C	79.37% (150/189)	78.3%	79.8%

clear that when the proposed moment variations or the original Legendre moments were used together with conventional features, the classification accuracy among bored and not bored trials increased significantly. In particular, the 85.19 percent CCR, produced by conventional features only, was increased up to 92.59 and 94.71 percent, when Legendre moments or the proposed moment variations (the Kr_{mod} GSR and Lg_{mod} IBI features) were, respectively, used together with the conventional features. These were expected results, following the analysis presented in Section 7.1, in which moments were found highly discriminative in respect of the specific classification problem. Furthermore, in the same section, it was shown that there were cases among the given data set (e.g., the "B3" GSR signal) where moments could discriminate well among bored and not bored trials, despite the fact that conventional features failed. As a result, the joint use of moments or the proposed moment variations with conventional features resulted in the correct classification of previously (using conventional features only) misclassified cases.

In the cases of $F_Set_CK_{mod}L_{mod}$ and F_Set_CLL , several conventional features initially selected from F_Set_C were replaced from different moment orders in the respective best selected feature sets. Also, in these cases, some new conventional features were chosen, not previously selected from F_Set_C . This indicates that moments and the proposed moment variations of different orders could possibly provide a better description of emotion-related biosignal characteristics than some conventional features. The combination of these moments with other conventional features could then boost ER accuracy.

At this point, it has to be noted that, for some of the extracted features, it was not possible to apply normalization based on each subject's baseline measurements; thus, in some cases, features and recorded signals were normalized on the basis of each subject's min and max values calculated or recorded. Although min-max normalization has the basic disadvantage that it cannot be trivially used toward on-the-fly emotion detection, it was used in this study since on-the-fly ER was not the immediate target. Another issue that comes up with min-max per-subject normalization is the fact that, when using LOOCV, information (the global min and max values calculated/recorded for the specific subject, common at the train and test sets) is transferred from the training set to each test case. This information transfer can be considered as capable of

artificially inflating the accuracy achieved. In our case, this fact could be thought to have further enhanced the accuracy of moment-based features in LOOCV. However, moment-based features also enhanced classification accuracy in LOSOCV by a max 10.05 percent where absolutely no information (global subject's min-max values) was shared between the train and test sets. This shows that information transferred in the present study's LOOCV analysis was not capable of standing for the gain in performance between the conventional and the moment-based features.

Regarding the 256 Hz sampling rate used for recording ECG and GSR signals during the experiment of this study, it has to be noted that although frequencies higher than 256 Hz have been used in the past (e.g., [3]), ECG and GSR sampling rates significantly lower than 256 Hz have also been successfully used in notable previous studies [5], [6] that derived HRV measures from ECG and extracted robust features from the GSR modality as well. In the present study, tests made prior to deploying the experiment showed that the 256 Hz sampling frequency allowed for the proper identification of R-peaks from the ECG and the extraction of robust features from the GSR signal in the specific application scenario. Furthermore, given the facts that 1) moment orders extracted in this work from GSR and IBI time series can be considered to assess information conveyed through frequencies below 1/4 of sampling rate and 2) prior to moment-based feature extraction signals had been subsampled at 4 Hz, the sampling rate of 256 Hz used can be considered as not to be influencing the moment-based feature calculation process at all.

Although a direct comparison of this study to previous ones is not possible due to the differences in the data sets and methodologies used, the results of two previous works can provide an indirect guide to point out the impact of the proposed approach. Chanel et al. reported in [18] a classification accuracy of 72.5 percent regarding the identification of boredom; an RBF SVM classifier was used, trained with conventional features extracted from GSR, blood pressure, and heart rate, respiration, and body temperature. Data were collected from 20 subjects and LOSOCV was employed. Rani et al. [19] achieved an 84.23 percent classification accuracy trying to identify three different intensity levels of boredom (low, medium, and high) by averaging classification results obtained from 15 subjects using LOOCV. Conventional features from ECG, GSR, bio-impedance, electromyogram, peripheral temperature, blood volume pulse, and heart sound were used.

Due to the facts that [18] and [19] used further monitoring modalities than ECG and GSR only, [18] following a LOSOCV methodology and [19] dealing with a three-class classification problem by following a subject-dependent perspective, a comparison between these two works and the present one could not be considered as valid. However, one could notice that even if [19] followed the more trivial subject-dependent methodology, the results obtained did not exceed 84.23 percent. Given the fact that [19] is the work with the highest accuracy reported in the literature regarding the automatic recognition of boredom from biosignal features, it is clear that there is a lot of space for improvements in the specific domain. One possible solution for improving the accuracy of such biosignals-based ER systems could be the utilization of further features in conjunction to the conventional ones. Moments as features with increased frequency resolution

capabilities can prove very helpful in this context. Following this line, in this work Krawtchouk and Legendre moments, as well as variations of them, used together with conventional features increased the initial classification accuracy obtained with conventional features only in the specific multisubject data set by a maximum 9.52 percent in LOOCV.

9 CONCLUSIONS

This paper presents work conducted toward the effective biosignals-based recognition of boredom, induced during video-game playing. In this context, the potentials of moments (Legendre and Krawtchouk) and novel variations of them as biosignal features toward automatic ER were for the first time examined. Initially, commonly used features were extracted from GSR and ECG data recorded from 19 subjects who participated in an experiment designed to induce boredom during playing a 3D Labyrinth video game. Using SBS on the initial conventional feature set and an LDA-based classifier (LOOCV), the player's self-reported boredom was predicted with a maximum accuracy of 85.19 percent. Then, by completely replacing the conventional GSR and IBI features with moments and the proposed moment variations and following the same classification procedure on the same data set, CCRs close to the initial one were achieved.

The best classification accuracies, however, were produced when the conventional features were fed together with moments or the proposed moment variations to the same LDA-based SBS feature selection process. Using conventional GSR and IBI features together with Legendre GSR and IBI moments boosted the accuracy of boredom recognition to 92.59 percent. Furthermore, when the conventional GSR and IBI features were used together with the proposed GSR Kr_{mod} and IBI Lg_{mod} ones as the initial feature set of SBS, a maximum CCR of 94.17 percent was obtained.

These findings indicate that moments like Legendre and Krawtchouk and, furthermore, the proposed moment variations are capable of coping with the complex nature of biosignals so as to capture characteristics of them related to human affective states. Indeed, a brief analysis conducted over some typical GSR signal cases addressed in this work showed that relatively low order moments can provide biosignal transformations of high discriminative power regarding the given problem, even in cases where conventional features totally fail. This was then further affirmed from the larger scale analysis followed, toward the automatic recognition of boredom, where the use of relatively low (up to the first 40) orders of moment-based features in conjunction with conventional ones was found to significantly increase classification accuracy. In the specific study, the utilized first 40 moment orders addressed signal frequencies up to approximately 0.8 Hz. Higher order moments would have addressed higher signal frequencies. However, these lower 40 orders addressing the specific low frequency range of GSR and IBI signals were found capable of significantly enhancing classification accuracy in the given application scenario.

Although the present work dealt with the specific, binary classification problem of boredom recognition over a specific data set derived from the experimental setup of this study, the results obtained can be considered as a strong indication that moments and moment variations can

be used in the future as helpful biosignal features toward the more accurate recognition of affective states. As was also shown in [6], more-than-two class affect recognition problems can be effectively split down to multiple two-class ones in order for better recognition accuracies to be achieved. Thus, enhancing the accuracy over a two-class classification problem could also lead in the future to better results in more-than-two class affect recognition works. Based on this work's findings, the joint use of moments and the proposed moment variations together with conventional features could enhance the accuracy of future biosignals-based emotion recognition systems.

REFERENCES

- [1] R.W. Picard, *Affective Computing*. MIT Press, 1997.
- [2] Z. Zeng, M. Pantic, G.I. Roisman, and T.S. Huang, "A Survey of Affect Recognition Methods: Audio, Visual, and Spontaneous Expressions," *IEEE Trans. Pattern Analysis and Machine Intelligence*, vol. 31, no. 1, pp. 39-58, Jan. 2009.
- [3] G. Chanel, J.J.M. Kierkels, M. Soleymani, and T. Pun, "Short-Term Emotion Assessment in a Recall Paradigm," *Int'l J. Human-Computer Studies*, vol. 67, no. 8, pp. 607-627, Aug. 2009.
- [4] R.R. Cornelius, *The Science of Emotion*. Prentice-Hall, 1996.
- [5] R.W. Picard, E. Vyzas, and J. Healey, "Toward Machine Emotional Intelligence: Analysis of Affective Physiological State," *IEEE Trans. Pattern Analysis and Machine Intelligence*, vol. 23, no. 10, pp. 1175-1191, Oct. 2001.
- [6] J. Kim and E. Andre, "Emotion Recognition Based on Physiological Changes in Music Listening," *IEEE Trans. Pattern Analysis and Machine Intelligence*, vol. 30, no. 12, pp. 2067-2083, Dec. 2008.
- [7] K.H. Kim, S.W. Bang, and S.R. Kim, "Emotion Recognition System Using Short-Term Monitoring of Physiological Signals," *Medical and Biological Eng. and Computing*, vol. 42, pp. 419-427, May 2004.
- [8] G. Chanel, J. Kronegg, D. Grandjean, and T. Pun, "Emotion Assessment: Arousal Evaluation Using EEG's and Peripheral Physiological Signals," *Proc. Int'l Workshop Multimedia Content Representation Classification and Security*, B. Günsel, A.M. Tekalp, A.K. Jain, and B. Sankur, eds., pp. 530-537, 2006.
- [9] C.L. Lisetti and F. Nasoz, "Using Noninvasive Wearable Computers to Recognize Human Emotions from Physiological Signals," *EURASIP J. Applied Signal Processing*, vol. 2004, pp. 1672-1687, Jan. 2004.
- [10] A. Haag, S. Goronzy, and P. Schaich, J. Williams, "Emotion Recognition Using Bio-Sensors: First Step toward an Automatic System," *Proc. Affective Dialog Systems: Tutorial and Research Workshop*, 2004.
- [11] J. Wagner, J. Kim, and E. André, "From Physiological Signals to Emotions: Implementing and Comparing Selected Methods for Features Extraction and Classification," *Proc. IEEE Int'l Conf. Multimedia and Expo*, 2005.
- [12] P. Rainville, A. Bechara, N. Naqvi, and A.R. Damasio, "Basic Emotions Are Associated with Distinct Patterns of Cardiorespiratory Activity," *Int'l J. Psychophysiology*, vol. 61, no. 1, pp. 5-18, 2006.
- [13] C.D. Katsis, N. Katertsidis, G. Ganiatsas, and D.I. Fotiadis, "Toward Emotion Recognition in Car-Racing Drivers: A Biosignal Processing Approach," *IEEE Trans. Systems, Man, and Cybernetics, Part A: Systems and Humans*, vol. 38, no. 3, pp. 502-512, May 2008.
- [14] P. Sundstrom, "Exploring the Affective Loop," PhD thesis, Stockholm Univ., 2005.
- [15] P. Sweetser and P. Wyeth, "GameFlow: A Model for Evaluating Player Enjoyment in Games," *ACM Computers in Entertainment*, vol. 3, p. 3, July 2005.
- [16] G.N. Yannakakis, M. Maragoudakis, and J. Hallam, "Preference Learning for Cognitive Modeling: A Case Study on Entertainment Preferences," *IEEE Trans. Systems, Man, and Cybernetics, Part A: Systems and Humans*, vol. 39, no. 6, pp. 1165-1175, Nov. 2009.
- [17] G.N. Yannakakis and J. Hallam, "Real-Time Game Adaptation for Optimizing Player Satisfaction," *IEEE Trans. Computational Intelligence and AI in Games*, vol. 1, no. 2, pp. 121-133, June 2009.
- [18] G. Chanel, C. Rebetez, M. Betrancourt, and T. Pun, "Boredom, Engagement and Anxiety as Indicators for Adaptation to Difficulty in Games," *Proc. 12th Int'l Conf. Entertainment and Media in the Ubiquitous Era*, 2008.
- [19] P. Rani, C. Liu, N. Sarkar, and E. Vanman, "An Empirical Study of Machine Learning Techniques for Affect Recognition in Human-Robot Interaction," *Pattern Analysis and Applications*, vol. 9, no. 1, pp. 58-69, 2006.
- [20] M.K. Hu, "Visual Pattern Recognition by Moment Invariants," *IRE Trans. Information Theory*, vol. 8, no. 2, pp. 179-187, Feb. 1962.
- [21] J. Shen, W. Shen, and D. Shen, "On Geometric and Orthogonal Moments," *Int'l J. Pattern Recognition and Artificial Intelligence*, vol. 14, no. 7, pp. 875-894, 2000.
- [22] M.R. Teague, "Image Analysis via the General Theory of Moments," *J. Optical Soc. of Am.*, vol. 70, no. 8, pp. 920-930, 1980.
- [23] S.M. Lajevardi and Z.M. Hussain, "Zernike Moments for Facial Expression Recognition," *Proc. Int'l Conf. Comm., Computer, and Power*, pp. 371-381, 2009.
- [24] C.H. Teh and R.T. Chin, "On Image Analysis by the Methods of Moments," *IEEE Trans. Pattern Analysis and Machine Intelligence*, vol. 10, no. 4, pp. 496-513, July 1988.
- [25] S. Li, M. Lee, and C. Pun, "Complex Zernike Moments Features for Shape-Based Image Retrieval," *IEEE Trans. Systems, Man, and Cybernetics, Part A: Humans and Systems*, vol. 39, no. 1, pp. 227-237, Jan. 2009.
- [26] P.-T. Yap, R. Paramesran, and S.-H. Ong, "Image Analysis by Krawtchouk Moments," *IEEE Trans. Image Processing*, vol. 12, no. 11, pp. 1367-1377, Nov. 2003.
- [27] B. Fu, J. Zhou, Y. Li, G. Zhang, and C. Wang, "Image Analysis by Modified Legendre Moments," *Pattern Recognition*, vol. 40, no. 2, pp. 691-704, Feb. 2007.
- [28] A. Mademlis, A. Axenopoulos, P. Daras, D. Tzovaras, and M.G. Strintzis, "3D Content-Based Search Based on 3D Krawtchouk Moments," *Proc. Third Int'l Symp. 3D Data Processing, Visualization, and Transmission*, 2006.
- [29] D. Ioannidis, D. Tzovaras, I.G. Damousis, S. Argyropoulos, and K. Moustakas, "Gait Recognition Using Compact Feature Extraction Transforms and Depth Information," *IEEE Trans. Information Forensics and Security*, vol. 2, no. 3, pp. 623-630, Sept. 2007.
- [30] G.G. Berntson, "Heart Rate Variability: Origins, Methods, and Interpretive Caveats," *Psychophysiology*, vol. 34, pp. 623-648, 1997.
- [31] Task Force of the European Soc. of Cardiology and the North Am. Soc. of Pacing and Electrophysiology, "Heart Rate Variability—Standards of Measurement, Physiological Interpretation, and Clinical Use," *Circulation*, vol. 93, no. 5, pp. 1043-1065, 1996.
- [32] J.L. Andreassi, *Psychophysiology: Human Behavior and Physiological Response*. Lawrence Erlbaum Assoc., 1995.
- [33] R.L. Mandryk and M.S. Atkins, "A Fuzzy Physiological Approach for Continuously Modeling Emotion During Interaction with Play Technologies," *Int'l J. Human-Computer Studies*, vol. 65, pp. 329-347, 2007.
- [34] G.Y. Yang, H.Z. Shu, C. Toumoulin, G.N. Han, and L.M. Luo, "Efficient Legendre Moment Computation for Gray Level Images," *Pattern Recognition*, vol. 39, no. 1, pp. 74-80, Jan. 2006.
- [35] R. Mukundan and K.R. Ramakrishnan, "Fast Computation of Legendre and Zernike moments," *Pattern Recognition*, vol. 28, no. 9, pp. 1433-1442, 1995.
- [36] G.-B. Wang; and S.-G. Wang; "Parallel Recursive Computation of the Inverse Legendre Moment Transforms for Signal and Image Reconstruction," *IEEE Signal Processing Letters*, vol. 11, no. 12, pp. 929-932, Dec. 2004.
- [37] R. Koekoek and R.F. Swarttouw, "The Askey-Scheme of Hypergeometric Orthogonal Polynomials and Its Q-Analogue," Faculty of Technical Math. and Informatics Report 98-17, Technische Univ. Delft, pp. 46-47, 1998.
- [38] P.A. Raj and A. Venkataramana, "Fast Computation of Inverse Krawtchouk Moment Transform Using Clenshaw's Recurrence Formula," *Proc. IEEE Int'l Conf. Image Processing*, pp. 37-40, 2007.
- [39] K.R. Scherer, "On the Nature and Function of Emotion: A Component Process Approach," *Approaches to Emotion*, K.R. Scherer and P. Ekman, eds., pp. 293-318, Lawrence Erlbaum Assoc., 1984.
- [40] K.R. Scherer, "Voice, Stress, and Emotion," *Dynamics of Stress*, M.H. Appley and R. Trumbull, eds., pp. 159-181, Plenum, 1986.
- [41] T.W. Malone, "What Makes Computer Games Fun?" *Byte*, vol. 6, pp. 258-277, 1981.
- [42] A. Jain and D. Zongker, "Feature Selection: Evaluation, Application, and Small Sample Performance," *IEEE Trans. Pattern Analysis and Machine Intelligence*, vol. 19, no. 2, pp. 153-163, Feb. 1997.



Dimitris Giakoumis received the diploma in electrical and computer engineering and the MSc degree in advanced computing and communication systems from Aristotle University of Thessaloniki in 2006 and 2008, respectively. He is a PhD student at Aristotle University of Thessaloniki, Greece, and a research associate in the Informatics and Telematics Institute of Thessaloniki. His main research interests include affective computing, biosignals processing, virtual and mixed reality, web services, and pervasive computing.



Dimitrios Tzovaras is a senior researcher (Grade A) in the Informatics and Telematics Institute of Thessaloniki and a visiting professor at the Imperial College London. Prior to his current position, he was a senior researcher in 3D imaging at Aristotle University of Thessaloniki. His main research interests include virtual reality, assistive technologies, 3D data processing, and stereo and multiview image sequence coding. His involvement with those research areas has led to the coauthoring of more than 60 papers in refereed journals and more than 150 papers in international conferences. He is a member of the IEEE.



Konstantinos Moustakas is currently a post-doctoral research fellow in the Informatics and Telematics Institute Centre for Research and Technology Hellas, Greece. He was also a visiting lecturer at Aristotle University of Thessaloniki during 2008. His main research interests include virtual reality, haptics, 3D content-based search, and computer vision. He is the (co)-author of more than 65 papers in refereed journals, edited books, and international conferences. He is a member of the IEEE and the IEEE Computer Society.



George Hassapis is a professor of computer architecture and industrial informatics and the director of the Laboratory of Computer System Architecture at Aristotle University of Thessaloniki, Greece. He has authored and coauthored more than 80 articles in refereed journals, conference proceedings, and book chapters and supervised many research projects funded by the European Union and Greek organizations. He is a senior member of the IEEE, a Chartered Engineer, and a recipient of awards from ABI and CBI.

▷ **For more information on this or any other computing topic, please visit our Digital Library at www.computer.org/publications/dlib.**